Ophthalmol Ther (2025) 14:2673–2695
https://doi.org/10.1007/s40123-025-01240-w

REVIEW

Retinal and Choroidal Changes in Transthyretin-Related Amyloidosis Using Optical Coherence Tomography Modalities: A Systematic Review

Makan Ziafati · Costanza Barresi · Chiara Giuffrè · Maria Vittoria Cicinelli

Received: July 11, 2025 / Accepted: August 29, 2025 / Published online: September 19, 2025

ABSTRACT

Introduction: Optical coherence tomography (OCT) and OCT angiography (OCT-A) are valuable tools for detecting retinal and choroidal changes in systemic diseases. This systematic review evaluates the current evidence on retinal and choroidal alterations associated with transthyretin-related amyloidosis (ATTR).

Methods: A systematic review was conducted in accordance with Preferred Reporting Items for Systematic Reviews and Meta-analyses (PRISMA) guidelines across PubMed, Scopus, Web of Science, and Embase up to December 2024 to investigate structural and microvascular alterations in the retina and choroid of patients with genetically confirmed ATTR, aiming to evaluate their potential as imaging biomarkers for disease monitoring.

Results: Nine eligible studies were identified, encompassing a total of 246 individuals, including both symptomatic patients and pre-symptomatic carriers. Reported findings included thinning of the outer nuclear layer (ONL), reduced vessel density in the superficial and deep capillary plexuses, enlargement of the foveal avascular zone (FAZ), and a decreased choroidal vascularity index (CVI).

Conclusions: Thinning of ONL was the most consistent structural finding, suggesting photoreceptor degeneration. Decreased CVI, reduced vascular density, and enlargement of the FAZ further indicate impaired vascular integrity. Although OCT and OCT-A show promise for early detection and monitoring of ocular involvement in ATTR, most studies were case–control studies with small sample sizes and possible confounding from ongoing treatments. These limitations highlight the need for standardized imaging protocols and longitudinal studies to confirm findings and clarify the link between ocular and systemic disease severity.

Supplementary Information The online version contains supplementary material available at https://doi.org/10.1007/s40123-025-01240-w.

M. Ziafati (✉)
Iranian Research Center for HIV/AIDS, Iranian Institute for Reduction of High-Risk Behaviors, Tehran University of Medical Sciences, Tehran, Iran
e-mail: makanziafati@gmail.com

M. Ziafati
Translational Ophthalmology Research Center, Farabi Eye Hospital, Tehran University of Medical Sciences, Tehran, Iran

C. Barresi · M. V. Cicinelli
School of Medicine, Vita-Salute San Raffaele University, Milan, Italy

C. Barresi · M. V. Cicinelli
Department of Ophthalmology, IRCCS San Raffaele Scientific Institute, Milan, Italy

C. Giuffrè
Centro Europeo Di Oftalmologia, Palermo, Italy

Keywords: Transthyretin-related amyloidosis; Retina; Choroid; Optical coherence tomography; Optical coherence tomography angiography

Key Summary Points

Why carry out this study?

Ocular involvement is a recognized but underexplored manifestation of transthyretin-related amyloidosis (ATTR). Optical coherence tomography (OCT) and OCT angiography (OCT-A) have shown potential in identifying structural and vascular alterations in the retina and choroid.

This systematic review aimed to synthesize available evidence on OCT and OCT-A findings in patients with genetically confirmed ATTR to assess their utility in clinical monitoring.

What was learned from the study?

This study identified consistent alterations in retinal and choroidal parameters among patients with ATTR, including outer nuclear layer (ONL) thinning, reduced vessel density in the superficial and deep capillary plexuses, enlargement of the foveal avascular zone (FAZ), and decreased choroidal vascularity index (CVI).

Findings suggest photoreceptor degeneration and microvascular compromise as key features of ocular ATTR.

INTRODUCTION

Amyloidosis encompasses a group of rare disorders characterized by extracellular deposition of insoluble protein fibrils with a β-pleated sheet configuration [1, 2]. These deposits may arise from acquired or hereditary conditions. Among the hereditary forms, familial amyloid polyneuropathy (FAP) is classified on the basis of the precursor protein, most commonly transthyretin (TTR), followed by apolipoprotein A-I and gelsolin [3]. TTR-related amyloidosis exists in two forms: variant (*ATTRv*), caused by *TTR* gene mutations, and wild-type (*ATTRwt*), which results from age-related misfolding of native TTR. *ATTRv* is the most prevalent hereditary amyloidosis [3, 4].

TTR is a transport protein for thyroxine (T4) and retinol (vitamin A), primarily synthesized in the liver, brain choroid plexus, and retinal pigment epithelium, where it plays a critical role in ocular metabolism [5–8]. *ATTRv* amyloidosis typically presents with peripheral neuropathy but can also affect the heart, kidneys, and eyes. Neurological symptoms result from TTR infiltration into the endoneurium due to blood–neural barrier disruption [9–12]. Conversely, *ATTRwt* primarily involves the heart, where TTR deposits cause restrictive cardiomyopathy and progressive heart failure. Although ocular involvement in *ATTRwt* has been less extensively characterized compared with *ATTRv*, recent studies indicate that it is relatively common and may even be more prevalent, with significant alterations involving both the anterior and posterior segments of the eye [8, 13–15].

Ocular involvement is a recognized and sometimes early feature of ATTR amyloidosis, arising from both hepatic and intraocular synthesis of mutant TTR. Affected structures may include the vitreous, iris, and retina [16–21]. In a large cohort study, Beirão et al. [22] reported scalloped iris in 27.9%, vitreous amyloidosis in 17.4%, and retinal angiopathy in 4.4% of carriers with *ATTRv* mutations. Similarly, Frizziero et al. [8] identified retinal pigment epithelium abnormalities—such as drusen and pigmentary changes—in 56% of patients with *ATTRwt* and 22% of patients with *ATTRv*. Vitreous opacities were also observed in 17% and 33% of patients with *ATTRwt* and *ATTRv*, respectively.

Advanced imaging modalities such as optical coherence tomography (OCT) and OCT angiography (OCT-A) have enhanced the ability to detect subtle retinal and choroidal changes in patients with ATTR [8, 14, 21].

Given the advent of disease-modifying therapies aimed at stabilizing or silencing TTR, there is an unmet need for reliable, noninvasive biomarkers to guide diagnosis and monitor therapeutic response [11, 23, 24]. This systematic review evaluates the utility of OCT and OCT-A

parameters as candidate imaging biomarkers in genetically confirmed ATTR amyloidosis, offering insight into the ocular pathophysiology of this multisystem disease [25].

METHODS

This systematic review was conducted in accordance with the Preferred Reporting Items for Systematic Reviews and Meta-analyses (PRISMA) guidelines [25]. The full list of search terms used is provided in the Electronic Supplementary Material (ESM). The study protocol was developed by one of the contributing authors and registered in the International Prospective Register of Systematic Reviews (PROSPERO; registration number CRD42024625522).

Study Selection

A comprehensive literature search was conducted in PubMed, Embase, Web of Science, and Scopus to identify relevant studies published up to December 2024. No geographical restrictions were applied. Two authors (M.Z. and C.B.) independently screened the titles and abstracts of all retrieved articles. Studies were included if they evaluated OCT or OCT-A parameters in patients with genetically confirmed hereditary ATTR. Irrelevant articles were excluded on the basis of title and abstract review; the full texts of the remaining articles were then assessed for eligibility.

Exclusion criteria were: (1) letters to the editor, reviews, or conference abstracts; (2) single-patient case reports; and (3) studies that did not assess OCT or OCT-A parameters. To ensure completeness, a manual search of reference lists from included articles was also performed. Disagreements were resolved through discussion.

Data Extraction

Two authors (M.Z. and C.B.) independently extracted data from the included studies. Extracted information included: first author's name, year of publication, study location, study design, and OCT/OCT-A device used.

Population characteristics were also recorded, including (1) sample size, (2) mean age, (3) sex distribution, (4) amyloidosis type (variant or wild-type), (5) specific gene mutations, (6) clinical manifestations, and (7) number of eyes with scalloped iris. Only OCT and OCT-A parameters reported in at least two studies were included in the analysis.

The following OCT parameters were extracted: central macular thickness (CMT), subfoveal choroidal thickness (SFCT), peripapillary retinal nerve fiber layer (pRNFL) thickness, and outer nuclear layer (ONL) thickness. OCT-A parameters included foveal avascular zone (FAZ) area and perimeter, vessel density (VD) in the superficial (SCP) and deep (DCP) capillary plexuses, perfusion density (PD), choriocapillaris (CC) vessel density, and choroidal vascularity index (CVI). The pRNFL was defined as the average RNFL thickness measured with a circumpapillary OCT scan centered on the optic nerve head; all other measurements were derived from scans centered on the macula.

Ethical Approval

This study is based on previously published literature and does not involve any new investigations involving human participants or animals; therefore, ethical approval was not required.

Quality Assessment

The methodological quality of the included studies was evaluated using the Newcastle–Ottawa Scale (NOS) for case–control and cohort studies and the National Institute of Health (NIH) quality assessment tools for cross-sectional and case series studies, which were independently applied to each article by two authors (M.Z. and C.B.) [26, 27]. Any discrepancies in the quality assessment were resolved through discussion with a third author (M.V.C.).

RESULTS

The study selection process is summarized in Fig. 1. A total of 313 records were identified

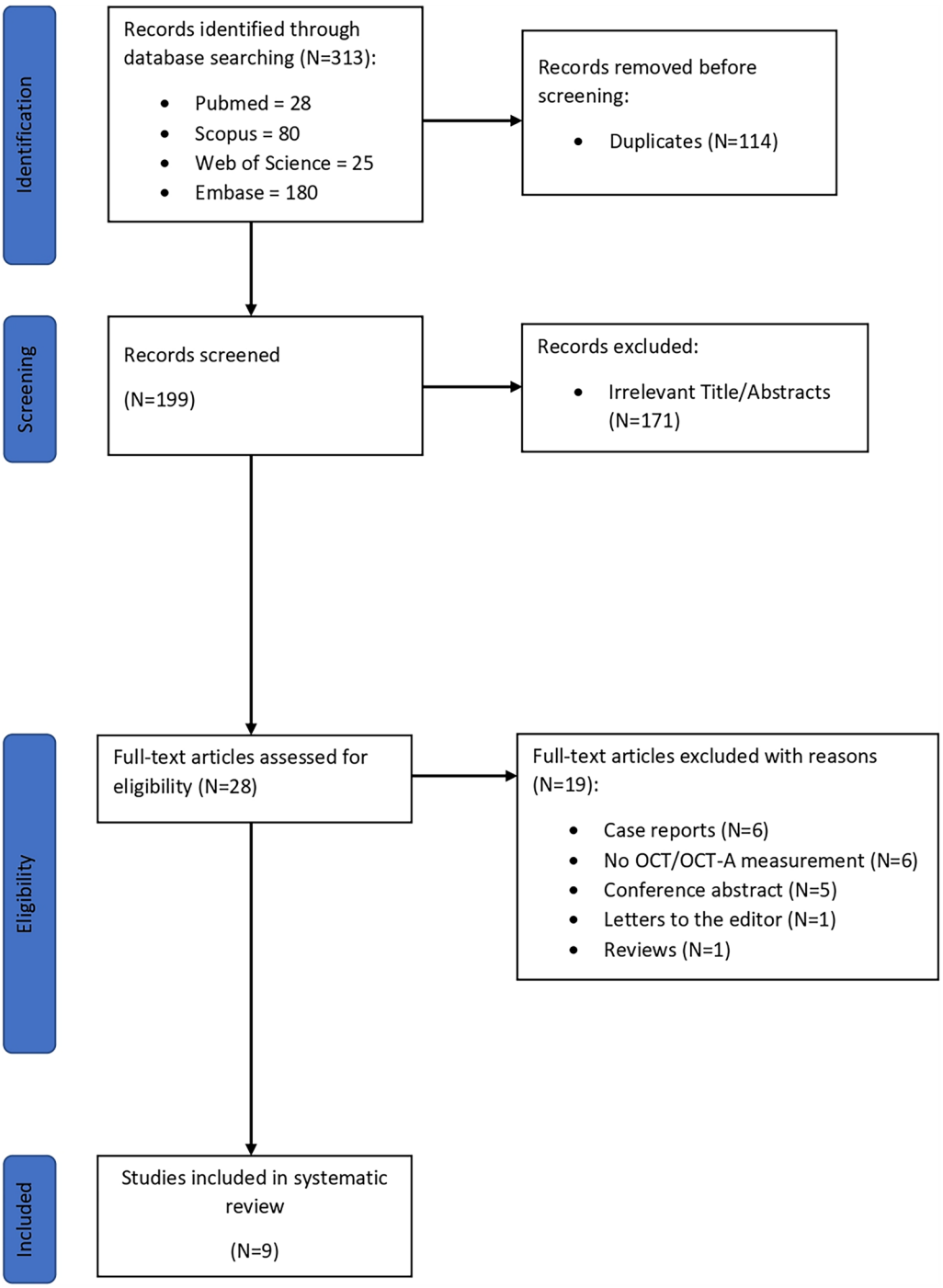

Fig. 1 PRISMA flow diagram illustrating the study selection process for the systematic review. *OCT* optical coherence tomography, *OCT-A* optical coherence tomography angiography

through electronic database searches: 28 from PubMed, 80 from Scopus, 25 from Web of Science, and 180 from Embase. After removing 114 duplicates, 199 unique records were screened. Following title and abstract review, 171 articles were excluded as irrelevant. The full texts of the

remaining 28 articles were assessed for eligibility. Of these, 19 were excluded for the following reasons: one was a letter to the editor, one a review article, five conference abstracts, six case reports, and six studies that did not assess OCT or OCT-A parameters. Ultimately, nine studies met the inclusion criteria and were included in the systematic review.

Characteristics of Studies

An overview of the included studies is presented in Tables 1 and 2. The studies were published between 2019 and 2023 and included a total of 246 patients, with sample sizes ranging from 9 to 166. Most participants were male (58.5%), and the mean age in ATTR groups ranged from 46.5 to 75.1 years.

Study designs varied and included five cross-sectional studies [5, 8, 28–30], two case–control studies [14, 21], and two case series [12, 31]. Most studies were conducted in Europe: four in Italy [8, 12, 14, 31], two in Portugal [21, 29], and one in Spain [30]. One study [28] was conducted outside Europe. Of the five studies [8, 12, 14, 21, 31] that included healthy control groups, three [8, 14, 21] applied age-matching, while the remaining two [12, 31] did not report any matching criteria related to age, sex, or race.

Regarding disease subtype, six studies focused on *ATTRv* [5, 12, 21, 28–30], one on *ATTRwt* [14], one on all ATTR types [8], and one [31] on presymptomatic carriers. OCT/OCT-A devices varied, including Heidelberg SPECTRALIS [8, 21, 30] (Heidelberg Engineering, Heidelberg, Germany), Zeiss Cirrus HD-OCT [5, 12, 31] (Carl Zeiss, Meditec, Inc., Dublin, CA, USA), Topcon DRI OCT [14] (Topcon Corporation, Japan), PLEX Elite 9000 [28] (Carl Zeiss Meditec, Inc., Dublin, CA, USA), and OptoVue AngioVue [32] (OptoVue, CA, USA). A variety of OCT and OCT-A imaging protocols were employed across the included studies. Most studies used macula-centered scans ranging from 3 × 3 mm to 6 × 6 mm.

Genetic mutation data were reported in seven studies [5, 8, 12, 28–31]. Most studies also documented treatment status, although two [5, 30] did not specify therapy type. Clinical manifestations (e.g., neuropathy, cardiomyopathy, and gastrointestinal involvement) were described in five studies [5, 8, 12, 14, 30], and scalloped iris was assessed in three [5, 21, 29].

Table 3 summarizes the OCT and OCT-A parameters reported across the included studies. SFCT and ONL thickness were manually measured. SFCT was defined as the distance from the posterior edge of the retinal pigment epithelium to the choroid–sclera junction, measured on horizontal OCT brightness scans (B-scans) using calipers. ONL thickness was measured at five predefined locations: at the fovea, and at 1500 µm and 3000 µm intervals nasal and temporal to the fovea, from the posterior edge of the outer plexiform layer to the external limiting membrane. Conversely, the FAZ area and perimeter, as well as CMT and pRNFL thickness, were all quantified using automated image analysis. All studies reporting vessel density in the SCP and DCP utilized automated measurements, except for Frizziero et al. [8], who calculated vessel density manually using the open-source ImageJ software (National Institutes of Health, Bethesda, MD, USA). PD was also assessed through automated methods.

Regarding choroidal parameters, CC vessel density was measured manually in the study by Frizziero et al. [8] In this study, the vascular-to-stromal (V/S) ratio was calculated using ImageJ software, with vessel density (V) defined as the proportion of the luminal choroidal area (LCA) (represented by white pixels) to the total choroidal area (TCA), and stromal density (S) defined as 1 – V, according to a previously described method [33]. In contrast, CC density was measured automatically in the study by Rinaldi et al. [14]. Both Rinaldi et al. and Marta et al. employed ImageJ software to calculate the CVI, where the TCA encompassed the entire selected region and the LCA was defined by the area occupied by hyporeflective vessels. CVI was then calculated as the ratio of LCA/TCA.

A meta-analysis was not conducted due to significant heterogeneity in the reporting of OCT and OCT-A parameters across the included studies. OCT-A metrics were assessed using diverse measurement scales and imaging protocols, preventing standardization necessary for quantitative pooling. Although structural parameters such as ONL and CMT were

Table 1 Characteristics of included studies

Studies	Country	Numbers of participants	Numbers of eyes	Sex (Male/Female)	Age (mean ± SD[a])	Amyloidosis	OCT/OCTA model	Study design
Frizziero et al. (2023)	Italy	ATTR 9	18	(8/1)	65.2 ± 13.4	*ATTRv*	Heidelberg Spectralis OCT	Cross-Sectional
		ATTR 17	34	(17/0)	75.1 ± 6.7	*ATTRwt*		
		ATTR 2	4	(2/0)	50.5 ± 2.1	Pre-symptomatic carriers		
		Control 49	98	(32/17)	66.2 ± 10.2	–		
Minnella et al. (2021)	Italy	ATTR 9	18	(6/3)	66.77 ± 13.40	*ATTRv*	Ziess Cirrus 5000 HD-OCT (spectral domain)	Case Series
		Control 13	26	(6/7)	NR	–		
Rinaldi et al. (2023)	Italy	ATTR 18	36	(14/4)	70.83 ± 6.33	*ATTRwt*	Topcon DRI OCT (SS)	Case–Control
		Control 16	32	(10/6)	68.81±9.01	–		
Maceroni et al. (2023)	Italy	ATTR 14	28	(5/9)	54.71 ± 13.69	Pre-symptomatic carriers	Ziess Cirrus 5000 HD-OCT (SD)	Case Series
		Control 13	26	(6/7)	NR	–		
Kakihara et al. (2022)	Japan	ATTR 36	36	(22/14)	51.8 ± 12.1	*ATTRv*	PLEX Elite 9000 OCTA (SS)	Cross-Sectional
Latasiewicz et al. (2019)	Spain	ATTR 8	15	(4/4)	57.13 ± 10.9	*ATTRv*	Ziess Cirrus HD-OCT	Cross-Sectional
Marques et al. (2020)	Portugal	ATTR 24	48	(15/9)	46.5 ± 5.0	*ATTRv*	OptoVue AngioVue OCTA	Cross-Sectional
Marta et al. (2022)	Portugal	ATTR 83	166	(36/47)	50.45 ± 8.31	*ATTRv*	Heidelberg Spectralis OCT	Case–Control
		Control 83	166	(NR)	50.47 ± 8.70	–		
Ruiz-Medrano et al. (2023)	Spain	ATTR 26	52	(15/11)	57.8 ± 13.7	*ATTRv*	Heidelberg Spectralis OCT	Cross-Sectional

EDI-OCT, [a] standard deviation abbreviations *ATTR* transthyretin-related amyloidosis, *ATTRv* transthyretin-related amyloidosis variant, *ATTRwt* transthyretin-related amyloidosis variant wild type, *EDI* enhanced depth imaging*NR* not reported, *OCT* optical coherence tomography, *OCTA* optical coherence tomography angiography, *SD* spectral domain,*SS* swept source

Table 2 Genetic mutations, treatment types, clinical features, and scan sizes in included studies

Studies	Mutations (*V30M*/Others)	Treatment (Tafamidis/Patisiran/Liver transplantation)	Clinical manifestations (Neuropathy/cardiomyopathy/gastrointestinal involvement)	Scalloped pupils (Eyes)	Amyloidosis	Scan size (mm)
Frizziero et al. (2023)	(2/7)	(5/4/0)	(8/6/NR)	NR	*ATTRv*	OCT: 6 × 6 OCTA: 3 × 3 & 6 × 6
	–	(1/0/0)	(7/17/NR)		*ATTRwt*	
	NR	–	–		Pre-symptomatic Carriers	
Minnella et al. (2021)	(3/6)	(5/3/0)	(8/5/4)	NR	*ATTRv*	6 × 6
Rinaldi et al. (2023)	–	(12/0/0)	(9/18/7)	NR	*ATTRwt*	6 × 6
Maceroni et al. (2023)	(5/10)	–	–	NR	Pre-symptomatic Carriers	6 × 6
Kakihara et al. (2022)	(30/6)	(10/7/17)	(NR/NR/NR	NR	*ATTRv*	3 × 3
Latasiewicz et al. (2019)	(5/3)	(NR/NR/5)	(3/5/2)	4	*ATTRv*	6 × 6
Marques et al. (2020)	(24/0)	(3/0/21)	(NR/NR/NR	24	*ATTRv*	3 × 3
Marta et al. (2022)	NR	(26/0/55)	(NR/NR/NR	92	*ATTRv*	6 × 6
Ruiz-Medrano et al. (2023)	(8/18)	(NR/NR/NR)[a]	(22/22/10)	NR	*ATTRv*	Radial 12-mm

[a]20/26 (76.9) received treatment. *ATTR*TTR amyloidosis, *ATTRv* transthyretin-related amyloidosis variant, *ATTRwt* transthyretin-related amyloidosis variant wild type, *V30M* Val30Met, *NR* not reported, *OCT* optical coherence tomography, *OCTA* optical coherence tomography angiography

reported more consistently, often stratified by different subtypes of ATTR. The clinical variability among these subtypes introduced substantial bias and limited the comparability of outcomes across studies.

ATTRv

Seven studies [5, 8, 12, 21, 28–30] evaluated retinal and choroidal changes in patients with ATTRv, focusing on parameters such as SFCT, pRNFL, CMT, ONL, vascular and perfusion density, FAZ, CC, and CVI.

Retinal Changes

Minnella et al. [12] demonstrated that both CMT and ONL were reduced in patients with *ATTRv* compared with healthy controls, with a statistically significant reduction observed only in ONL thickness.

Table 3 OCT/OCTA parameters reported in each study

Studies	Country	CMT	SFCT	pRNFL	ONL	FAZ area	FAZ perimeter	SCP VD	DCP VD	PD	CC VD	CVI
Frizziero (2023)	Italy	NR	NR	R	NR	NR	NR	R	R	NR	R[a]	NR
Minnella (2021)	Italy	R	R	NR	R	NR	NR	NR	NR	NR	NR	NR
Rinaldi (2023)	Italy	NR	NR	NR	NR	NR	NR	R	R	NR	R	R
Maceroni (2023)	Italy	R	R	R	R	R	R	R	NR	R	NR	NR
Kakihara et al. (2022)	Japan	NR	NR	NR	NR	R	NR	R	R	R	NR	NR
Latasiewicz et al. (2019)	Spain	NR	R	NR	NR	R	NR	NR	NR	NR	NR	NR
Marques et al. (2020)	Portugal	NR	NR	NR	NR	R	R	R	R	NR	NR	NR
Marta et al. (2022)	Portugal	NR	NR	NR	NR	NR	NR	NR	NR	NR	NR	R
Ruiz-Medrano et al. (2023)	Spain	NR	R	R	NR	NR	NR	NR	NR	NR	NR	NR

[a] Reported as vascular-to-stromal ratio. *CC* choriocapillaris, *CMT* central macular thickness, *CVI* choroidal vascularity index, *DCP* deep capillary plexus, *FAZ* foveal avascular zone, *NR* not reported, *OCT* optical coherence tomography, *OCT-A* optical coherence tomography angiography, *ONL* outer nuclear layer, *PD* perfusion density, *pRNFL* peripapillary retinal nerve fiber layer, *R* reported, *SCP* superficial capillary plexus, *SFCT* subfoveal choroidal thickness, *VD*, vessel density

pRNFL was evaluated in two studies. Frizziero et al. [8] found no difference between patients with *ATTRv* and controls, while Ruiz-Medrano et al. [30] reported thinner pRNFL in patients with more severe cardiac involvement.

Vessel density in the SCP and DCP was assessed in three studies. Frizziero et al. [8] reported significant reductions in macular and peripapillary VD. Kakihara et al. [28] found no association between VD and systemic severity, which was defined as the sum of organ-specific scores ranging from 0 (no impairment) to 3 (severe disability or organ transplantation. Marques et al. [29] observed significantly lower SCP and DCP VD in eyes with scalloped iris compared with those without.

FAZ area was evaluated in three studies. Kakihara et al. [28] and Latasiewicz et al. [5] found no significant differences compared with controls and no correlation with systemic severity, while Marques et al. [29] reported a larger FAZ area and perimeter in eyes with scalloped iris.

Choroidal Changes

SFCT was assessed in three studies. Minnella et al. [12] reported a nonsignificant reduction in SFCT in patients with *ATTRv* compared with controls. Moreover, Latasiewicz et al. [5] and Ruiz-Medrano et al. [30] observed decreased SFCT relative to age-matched populations.

Two studies reported choroidal measurements in patients with *ATTRv*. Frizziero et al. [8] found significantly reduced vascular density in the choriocapillaris in patients with *ATTRv*. Marta et al. [21] reported a significantly lower CVI in patients with *ATTRv* compared with controls (Table 4).

ATTRwt

Two studies [8, 14] examined retinal and choroidal changes in patients with *ATTRwt*.

Retinal Changes

Frizziero et al. [8] reported significant thinning of pRNFL in patients with *ATTRwt* compared with controls, especially in the temporal and inferior temporal sectors, with greater thinning than in *ATTRv* and presymptomatic carriers.

Both studies found significantly reduced SCP and DCP VD in patients with *ATTRwt* across all Early Treatment Diabetic Retinopathy Study (ETDRS) sectors. Rinaldi et al. [14] observed consistent reductions in all quadrants, aligning with findings from Frizziero et al.

Choroidal Changes

Both studies reported lower CC vascular density in patients with *ATTRwt* compared with healthy controls. Frizziero et al. [8] noted that CC density in patients with *ATTRwt* was lower than in *ATTRv* and presymptomatic carriers, suggesting more severe choroidal involvement. Rinaldi et al. [14], who evaluated CVI, found a reduction in patients with *ATTRwt* that did not reach statistical significance (Table 5).

Pre-symptomatic Carriers

OCT/OCT-A findings in presymptomatic TTR mutation carriers were assessed in two studies.

Retinal Changes

Maceroni et al. [31] reported reduced CMT and ONL in carriers, with no significant changes in SFCT or pRNFL. Frizziero et al. [8] also found no difference in pRNFL compared with controls. Both studies evaluated SCP VD and found no significant differences. DCP VD was reported only by Frizziero et al. [8], also showing no difference.

Maceroni et al. [31] found reduced PD in carriers, though not statistically significant. Only Maceroni et al. [31] assessed FAZ, reporting larger FAZ area and perimeter in carriers, again without statistical significance.

Choroidal Changes

Only Frizziero et al. [8] assessed choroidal parameters in carriers and reported no significant

Table 4 OCT/OCT-A findings in patients with ATTRv

Structure	Study	Numbers of participants	OCT/OCT-A measurement	Findings
Retinal	Minnela et al.	ATTR 9 Control 13	SFCT, CMT, ONL	In patients with *ATTRv*, CMT and SFCT were slightly lower (257.33 ± 24.46 μm and 272.22 ± 60.68 μm, respectively) compared with the control group (264.57 ± 13.36 μm and 278.80 ± 37.92 μm, respectively); however, these differences did not reach statistical significance (both $P > 0.05$). In contrast, ONL thickness demonstrated a statistically significant reduction in patients with *ATTRv* compared with controls (72.57 ± 8 μm versus 79.5 ± 6.05 μm, $\boldsymbol{P = 0.002}$).
	Latasiewicz et al.	ATTR 8	SFCT, FAZ area	Across all three age groups, SFCT was consistently lower in both eyes compared with the healthy controls reported by Yavuzer et al. [34]. In individuals aged 40–49 years, SFCT was measured at 284.5 ± 8.5 μm in the right eye and 240 ± 0 μm in the left eye, whereas the corresponding values in healthy controls were notably higher, at 309.85 ± 60.05 μm and 318.06 ± 67.01 μm, respectively. A similar trend was observed in the 50–59 years age group, where SFCT values were 267 ± 35 μm in the right eye and 241 ± 3 μm in the left eye, in comparison to 278.88 ± 51.29 μm and 285.06 ± 49.52 μm, respectively, among healthy individuals. The reduction in SFCT was also noted in the 60–73 years age group, where the right and left eyes exhibited thickness values of 225 ± 37.23 μm and 188 ± 24.91 μm, respectively, compared with 266.50 ± 49.56 μm and 256.00 ± 55.55 μm in the control group. In the study, the mean FAZ was similar to the reported in healthy subjects [35, 36]: 0.27 ± 0.11 mm^2 to 0.329 ± 0.115 mm^2.

Table 4 continued

Structure	Study	Numbers of participants	OCT/OCT-A measurement	Findings
	Ruiz-Medrano et al.	ATTR 26	SFCT, pRNFL	The study found an SFCT of 227.8 ± 76.5 μm, lower than in healthy controls reported by Yavuzer et al. [34]. Furthermore, greater cardiac involvement correlated with reduced pRNFL thickness (***P*** **< 0.05**).
	Frizziero et al.	ATTR 9 Control 49	pRNFL, SCP VD, DCP VD	In patients with *ATTRv*, the pRNFL thickness (100.5 ± 9.3 μm) was lower than healthy controls (103.3 ± 8.5 μm, ***P*** **< 0.05**). Moreover, both the SCP VD (0.2847 ± 0.1216 μm) and DCP VD (0.1475 ± 0.0918 μm) were reduced compared with controls (0.394 ± 0.062 μm and 0.249 ± 0.081 μm, respectively)(both ***P*** **< 0.05**).
	Kakihara et al.	ATTR 36	SCP VD, DCP VD, PD, FAZ area	The systemic severity score showed no significant correlation with superficial, deep, or total retinal perfusion density ($r = -0.0302$, $P = 0.861$; $r = -0.0737$, $P = 0.669$; $r = -0.0717$, $P = 0.678$, respectively). Likewise, no significant association was found between the systemic severity score and superficial, deep, or total retinal vessel density ($r = -0.0677$, $P = 0.695$; $r = -0.100$, $P = 0.561$; $r = -0.0780$, $P = 0.651$, respectively). Additionally, the severity score did not correlate with FAZ size ($r = 0.086$, $P = 0.617$).
	Marques et al.	ATTR 24	SCP VD, DCP VD, FAZ area, FAZ perimeter	Patients with *ATTRv* who exhibit a scalloped iris present with a diminished retinal vascular network, as evidenced by an enlarged FAZ area (Δ = 0.02 ± 0.03 mm^2, ***P*** **= 0.002**) and perimeter (Δ = 0.15 ± 0.20 mm, ***P*** **= 0.002**). Additionally, this group exhibits vascular density changes, including reductions in both superficial capillary density (Δ = −1.50% ± 3.52%, ***P*** **= 0.049**) and deep capillary density (Δ = −2.53% ± 5.08%, ***P*** **= 0.023**).

Table 4 continued

Structure	Study	Numbers of participants	OCT/OCT-A measurement	Findings
Choroid	Frizziero et al.	ATTR 9 Control 49	CC	The CC vascularity in patients with *ATTRv* is lower compared with healthy controls (0.5901 ± 0.1682 versus 0.704 ± 0.135) (***P* < 0.05**).
	Marta et al.	ATTR 83 Control 83	CVI	The study revealed that the CVI within the 5 mm-width area was significantly lower in patients with *ATTRv* ($71.41\% \pm 3.84\%$) compared with healthy controls ($75.80\% \pm 3.31\%$) (***P* < 0.001**).

ATTR transthyretin-related amyloidosis, *ATTRv* transthyretin-related amyloidosis variant, *CC* choriocapillaris, *CMT* central macular thickness, *CVI* choroidal vascularity index, *DCP* deep capillary plexus, *FAZ* foveal avascular zone, *OCT* optical coherence tomography, *OCT-A* optical coherence tomography angiography, *ONL* outer nuclear layer, *PD* perfusion density, *pRNFL* peripapillary retinal nerve fiber layer, *SCP* superficial capillary plexus, *SFCT* subfoveal choroidal thickness, *VD* vessel density

differences in CC vascular components compared with controls (Table 6).

Quality Assessment

The quality assessment of the included studies indicated overall moderate to high methodological rigor across the different study designs. The case–control studies were of high quality, characterized by clearly defined cases, representative sampling, and consistent exposure assessment, although reporting on control selection was limited. The case series studies also demonstrated strong quality, with well-defined objectives, clearly described populations, and reliable outcome measures. Cross-sectional studies generally fulfilled key quality criteria, including clearly stated objectives and valid, consistently applied outcome assessments (ESM) [35, 36].

DISCUSSION

Retinal and Choroidal Imaging

This systematic review reveals consistent retinal and choroidal alterations in patients with ATTR, as assessed by OCT and OCT-A (Table 1). Retinal involvement in ATTR was first reported by Falls et al. [37] in 1955, and subsequent studies have expanded on these observations. Two studies assessed pRNFL thickness: Maceroni et al. found a nonsignificant reduction in pre-symptomatic carriers, whereas Frizziero et al. observed generalized thinning, particularly in patients with *ATTRwt*. This thinning may reflect age-related degeneration or more extensive amyloid deposition within retinal ganglion cells, especially in the native (wild-type) form of TTR, which lacks the conformational changes of mutant TTR and tends to deposit more broadly in the retina [4, 7, 8, 11, 31, 38].

ONL thinning was a consistent finding in both patients with *ATTRv* and pre-symptomatic carriers. This may be attributed to impaired retinoid metabolism, ultimately affecting photoreceptor integrity. Supporting this hypothesis, Minnella et al. reported corresponding reductions in scotopic and photopic electroretinogram responses in patients with ATTR, indicating that ONL thinning reflects both structural and functional photoreceptor compromise. These findings position ONL thickness as a promising structural biomarker of retinal involvement in ATTR [12]. CMT and SFCT showed variable findings. CMT was

significantly reduced in pre-symptomatic carriers but remained comparable to controls in patients with *ATTRv*. SFCT, by contrast, was consistently decreased in patients with *ATTRv* but not significantly different between carriers and controls. These inconsistencies may reflect differences in disease stage, subtype, or the limited sample sizes of individual studies. Vessel density within the SCP and DCP was notably reduced in *ATTRv* and *ATTRwt* groups, while pre-symptomatic carriers demonstrated SCP vessel densities similar to controls (Fig. 2).

Retinal angiopathy (RA), often presenting as microaneurysms and hemorrhages, has been well documented in ATTR. Several pathophysiological mechanisms have been proposed. First, perivascular amyloid sheathing may cause occlusive arteriolar changes, leading to peripheral ischemia and, in severe cases, neovascularization. Histological studies confirm perivascular amyloid deposits in retinal tissues [37, 39–43]. Second, oligomeric TTR aggregates are known to damage vascular endothelial tight junctions, disrupting barrier function and promoting microaneurysm formation and hemorrhage [9, 44]. Rousseau and colleague [41] reported microaneurysms in all eyes examined and retinal hemorrhages in several patients, highlighting the clinical significance of this mechanism.

Third, amyloid may directly infiltrate retinal vasculature, akin to its behavior in cerebral amyloid angiopathy and oculoleptomeningeal amyloidosis [45–47]. Fourth, systemic disease—including cardiac and pulmonary involvement—may impair oxygen delivery to the retina, exacerbating ischemia and contributing to FAZ enlargement and, ultimately, neovascular glaucoma [48–51]. Although FAZ area and perimeter were larger in patients with *ATTRv* and pre-symptomatic carriers in some studies [5, 31], these findings did not reach statistical significance, likely due to limited sample sizes.

Notably, the presence of a scalloped iris was associated with more severe subclinical retinal angiopathy in *ATTRv* eyes, as shown by Marques et al. [29], suggesting it may serve as a useful clinical marker for retinal involvement.

Choroidal changes were also frequently reported. The CVI, reflecting the ratio of vascular luminal area to total choroidal area, was significantly reduced in patients with *ATTRv*. This reduction likely results from stromal amyloid deposition disrupting choroidal perfusion. Similar findings were observed in patients with *ATTRwt*, although the reduction in CVI did not always reach statistical significance. The CC vascular density was also decreased in both ATTR subtypes, reinforcing the concept of choroidal involvement. Findings suggest that CVI, particularly when combined with retinal biomarkers such as ONL or SCP/DCP vessel density, could serve as a valuable imaging biomarker of ATTR-related ocular disease [5, 14, 21, 52].

Genetic Mutations

Seven of the included studies reported mutation-specific data [5, 8, 12, 28–31]. The *Val30Met* (*V30M*) mutation was the most prevalent and is also the most frequently associated with ocular involvement worldwide [53, 54]. However, the prevalence of ocular findings in *V30M* carriers varies widely by region. For example, Beirão et al. [22] reported retinal angiopathy in only 4% of Portuguese *V30M* carriers, while Reynolds et al. [16] found ocular involvement in 8 of 54 patients in a US cohort. In contrast, Kakihara et al. [55] reported RA in 37.5% of Japanese *V30M* eyes, underscoring the potential role of environmental or genetic modifiers.

Other mutations, such as *Ala36Pro* and *Phe64Leu*, have also been linked to a high prevalence of ocular findings [56–59]. The relatively high frequency of *Phe64Leu* in this review reflects its predominance in the Italian population [60], where several included studies were conducted. Future genotype–phenotype correlation studies are needed to determine whether specific mutations confer greater risk for retinal or choroidal involvement.

Clinical Manifestations

Cardiomyopathy was the most frequently reported systemic feature [13, 61], especially in patients with *ATTRwt*, followed by neuropathy. Ruiz-Medrano et al. [30] found that patients with ocular amyloidosis also exhibited more

Table 5 OCT/OCT-A findings in patients with ATTRwt

Structure	Study	Numbers of participants	OCT/OCT-A measurement	Findings
Retinal	Frizziero et al.	ATTR 17 Control 13	pRNFL, SCP VD, DCP VD	Patients with *ATTRwt* exhibited a significantly lower pRNFL thickness compared with healthy controls (83.9 ± 17.1 μm versus 103.3 ± 8.5 μm). Additionally, pRNFL thickness in patients with *ATTRwt* was lower than in those with *ATTRv* (100.5 ± 9.3 μm) and carriers (106.3 ± 8.7 μm). A comparison among groups (*ATTRwt*, *ATTRv*, and carriers) revealed a significant difference in global peripapillary RNFL thickness, particularly in the temporal and temporal inferior sectors (***P* = 0.0413**, ***P* = 0.0205**, and ***P* = 0.0009**, respectively). patients with *ATTRwt* demonstrated the lowest pRNFL thickness, with statistically significant reductions in the temporal inferior sector compared with *ATTRv* (***P* = 0.0059**) and carriers (***P* = 0.0053**). Furthermore, patients with *ATTRwt* showed significantly lower vascular density in both the SCP (0.2557 ± 0.0837 versus 0.394 ± 0.062) and DCP (0.1278 ± 0.0646 versus 0.249 ± 0.08).
	Rinaldi et al.	ATTR 18 Control 16	SCP VD, DCP VD	Across all sectors, patients with *ATTRwt* showed significantly lower vessel density in both the SCP and DCP compared with healthy controls (all ***P* < 0.05**): Central mVD (%): 15.66 ± 3.59 versus 19.41 ± 1.61 for SCP and 23.45 ± 4.72 versus 28.45 ± 2.68 for DCP. Inferior (%): 31.85 ± 7.51 versus 43.24 ± 4.11 for SCP and 31.21 ± 9.57 versus 44.36 ± 3.36 for DCP. Superior (%): 32.18 ± 7.16 versus 42.12 ± 3.67 for SCP and 32.59 versus 43.98 for DCP. Nasal (%): 33.55 ± 5.34 versus 40.43 ± 3.45 for SCP and 33.74 ± 6.86 versus 43.42 ± 2.95 for DCP. Temporal (%): 33.13 ± 7.81 versus 40.70 ± 2.64 for SCP and 33.58 ± 8.33 versus 43.92 ± 2.30 for DCP.

Table 5 continued

Structure	Study	Numbers of participants	OCT/OCT-A measurement	Findings
Choroid	Frizziero et al.	ATTR 17 Control 13	CC	They found that vascular/stroma density ratio of CC in patients with *ATTRwt* is lower than healthy control (0.4603 ± 0.1423 versus 0.704 ± 0.135) (***P* < 0.05**).
	Rinaldi et al.	ATTR 18 Control 16	CC, CVI	The study revealed that vessel density in patients with *ATTRwt* was significantly lower than healthy controls across all ETDRS sectors (all ***P* < 0.05**): Central mVD (%): 25.67 ± 4.33 versus 45.71 ± 5.08. Inferior (%): 42.23 versus 51.38. Superior (%): 40.66 versus 49.46. Nasal (%): 42.88 versus 50.06. Temporal (%): 42.02 versus 50.38. In contrast, the CVI was comparable between the two groups (32.86 versus 41.57, $P > 0.05$).

ATTR transthyretin-related amyloidosiss, *ATTRv* transthyretin-related amyloidosis variant, *ATTRwt* transthyretin-related amyloidosis wild type, *CC* choriocapillaris, *CVI* choroidal vascularity index, *DCP* deep capillary plexus, *ETDRS* Early Treatment Diabetic Retinopathy Study, *mVD* mean vessel density, *OCT* optical coherence tomography, *OCT-A* optical coherence tomography angiography, *pRNFL* peripapillary retinal nerve fiber layer, *SCP* superficial capillary plexus, *VD* vessel density

severe cardiac and neurological involvement, and that pRNFL thinning correlated with elevated cardiac biomarkers (troponin and creatinine) and reduced visual acuity. Carpal tunnel syndrome (CTS) is also common, particularly in patients with *ATTRwt* [62, 63]. Campagnolo et al. [64] found CTS in the majority of *ATTRwt* cases on electrodiagnostic testing. Corneal confocal microscopy has emerged as a noninvasive tool for detecting small fiber neuropathy in ATTR. Both Frizziero et al. [8] and Rousseau et al. [65] reported significantly reduced corneal nerve fiber length (CNFL) and increased stromal nerve tortuosity in patients with ATTR. Therefore, CNFL may serve as an ocular biomarker of peripheral neuropathy in ATTR.

Gastrointestinal symptoms were also frequently reported, particularly in early-onset *V30M* carriers, with weight loss and early satiety being common. The Transthyretin Amyloidosis Outcomes Survey (THAOS) confirmed high rates of gastrointestinal (GI) disturbances in patients with ATTR, particularly in *V30M*-associated disease [66–68]. Kakihara et al. [28] investigated correlations between OCT-A parameters and systemic severity scores, but found no significant associations. This suggests that retinal biomarkers may reflect localized pathology more than overall disease burden (Fig. 3).

Treatment

Six studies [8, 12, 14, 21, 28, 29] included patients treated with tafamidis, a TTR stabilizer that binds with high affinity to the thyroxine-binding sites of the TTR tetramer and prevents its dissociation into monomers—a critical step in the pathogenic cascade, as native TTR normally circulates as a tetramer, and its dissociation leads to intermediates that misassemble into amyloid fibrils [69–72]. Tafamidis has demonstrated efficacy in managing neuropathy and cardiomyopathy [73–75] but does not cross the blood–brain

Table 6 OCT/OCT-A findings in pre-symptomatic carriers

Structure	Study	Numbers of participants	OCT/OCT-A measurement	Findings
Retinal	Frizziero et al.	ATTR 17 Control 13	pRNFL, SCP VD, DCP VD	Pre-symptomatic patients demonstrated pRNFL thickness comparable to healthy controls (106.3 ± 8.7 μm versus 103.3 ± 8.5 μm, $P > 0.05$). Moreover, vessel density in both the superficial and deep capillary plexuses did not differ significantly between pre-symptomatic patients and healthy controls (0.4275 ± 0.0838 versus 0.394 ± 0.062 and 0.2243 ± 0.0458 versus 0.249 ± 0.081, respectively) ($P > 0.05$).
	Maceroni et al.	ATTR 18 Control 16	CMT, ONL, SFCT, pRNFL, SCP VD, FAZ area, FAZ perimeter, PD	In pre-symptomatic carriers, CMT was significantly reduced compared with healthy controls (251.35 ± 18.05 μm versus 266.15 ± 11.61 μm, $\mathbf{P = 0.01}$), whereas SFCT showed no difference between the groups (270.85 ± 68.77 μm versus 270.38 ± 36.75 μm, $P = 0.9$). Similarly, ONL thickness was significantly lower in pre-symptomatic carriers than in normal controls (67.5 ± 5.98 μm versus 79.87 ± 5.5 μm, $\mathbf{P = 0.01}$). The mean pRNFL thickness in pre-symptomatic carriers was 94 ± 8.7 μm, which did not differ significantly from normal controls. Although not reaching statistical significance, pre-symptomatic carriers exhibited an attenuated superficial retinal vascular network compared with healthy controls, characterized by a reduction in vessel density (17.5 ± 0.7 versus 18.86 ± 0.8 mm/mm^2, $P = 0.05$) and PD (42.77% ± 5.5% versus 45.7% ± 1.7%, $P = 0.08$). Additionally, pre-symptomatic carriers demonstrated a larger FAZ area (0.30 ± 0.1 versus 0.23 ± 0.07 mm^2, $P = 0.4$) and FAZ perimeter (2.24 ± 0.4 versus 2.09 ± 0.5 mm, $P = 0.4$), though these differences were not statistically significant.
Choroid	Frizziero et al.	ATTR 17 Control 13	CC	Pre-symptomatic carriers show no difference in vascular-to-stromal density of the CC compared with healthy controls (0.8018 ± 0.2286 versus 0.704 ± 0.135, *P-value* > 0.05).

Table 6 continued

ATTR transthyretin-related amyloidosis, *CC* choriocapillaris, *CMT* central macular thickness, *DCP* deep capillary plexus, *FAZ* foveal avascular zone, *OCT* optical coherence tomography, *OCT-A* optical coherence tomography angiography, *ONL* outer nuclear layer, *PD* perfusion density, *pRNFL* peripapillary retinal nerve fiber layer, *SCP* superficial capillary plexus, *SFCT* subfoveal choroidal thickness, *VD* vessel density

or blood–retinal barriers [76, 77], raising doubts about its effect on ocular manifestations. Patisiran, a small interfering RNA, harnesses RNA interference to silence *TTR* gene expression by targeting the 3′ untranslated region of *TTR* mRNA, thereby reducing both mutant and wild-type TTR production [78, 79] and leading to systemic benefits in patients with ATTR, including improved neuropathy [78, 80–82] and cardiac function [83, 84]; however, its ocular effects remain unclear. Dedicated trials are needed to assess whether patisiran impacts retinal or choroidal involvement.

Liver transplantation (LT) was the first disease-modifying intervention for ATTR, aimed at eliminating the hepatic source of mutant TTR [85, 86]. While highly effective in early-onset *V30M* cases, LT is less successful in non-*V30M* or late-onset variants [87]. Moreover, ocular manifestations often progress post-transplantation, likely due to intraocular synthesis of mutant TTR by the retinal and ciliary pigment epithelium [20,

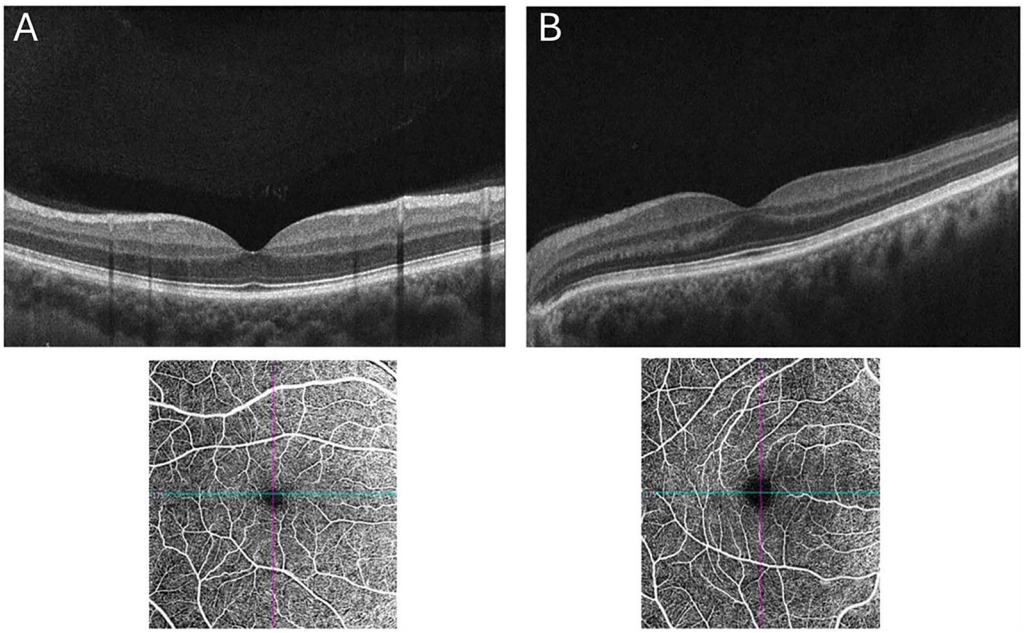

Fig. 2 From top to bottom, the figure presents OCT B-scan and OCT-A images of the SCP in a healthy control **A** and a pre-symptomatic carrier of *ATTRv* **B** In panel A, the OCT B-scan demonstrates preserved retinal layer morphology and reflectivity, with a mean ONL thickness of 79 μm. The corresponding OCT-A en face image of the SCP shows a vessel density of 19.8 mm/mm^2. In panel B, the OCT B-scan of the *ATTRv* carrier similarly displays intact retinal structure and reflectivity, with a mean ONL thickness of 61 μm and SCP vessel density measured at 17 mm/mm^2. Reprinted from Maceroni M, Falsini B, Luigetti M, et al. "Ocular Morpho-Functional Evaluation in ATTRv Pre-symptomatic Carriers: A Case Series." *Diagnostics*. 2023;13 (3). Creative Commons [31]. Abbreviations: *ATTRv* transthyretin-related amyloidosis variant, *B-scan* brightness scan, *OCT* optical coherence tomography, *OCT-A* optical coherence tomography angiography, *ONL* outer nuclear layer, *SCP* superficial capillary plexuses, *VD* vessel density

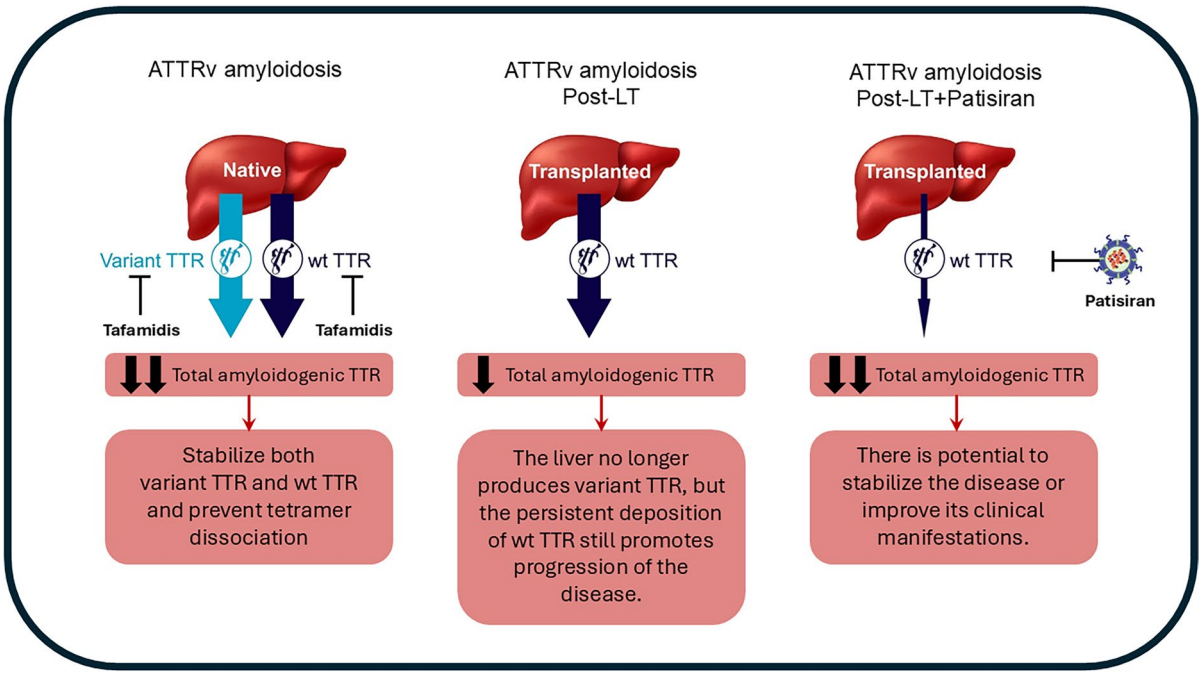

Fig. 3 Overview of therapeutic strategies in *ATTRv*. Tafamidis is a small-molecule stabilizer that binds to and stabilizes both variant and wild-type (wt) TTR, preventing tetramer dissociation. Liver transplantation eliminates the hepatic source of variant TTR, but continued deposition of wt TTR can lead to disease progression post-transplant. Patisiran, an RNA interference therapeutic, suppresses hepatic production of both variant and wt TTR and can be used either as first-line therapy or following LT. This dual suppression may result in stabilization or improvement of clinical manifestations Adapted from Schmidt HH, Wixner J, Planté-Bordeneuve V, et al. "Patisiran treatment in patients with hereditary transthyretin-mediated amyloidosis with polyneuropathy after liver transplantation." *Am J Transplant*. 2022;22(6):1646–1657. Creative Commons [93]. Abbreviations: *ATTRv* transthyretin-related amyloidosis variant, *LT* liver transplantation, *TTR* transthyretin, *wt* wild-type

88–92]. Thus regular ophthalmologic monitoring is needed even after systemic treatment.

This review represents the first systematic evaluation of OCT and OCT-A findings in ATTR amyloidosis. Nevertheless, several limitations should be considered. Most included studies were cross-sectional or case–control in design, precluding longitudinal assessment of disease progression. Small sample sizes and heterogeneous imaging protocols limit generalizability and may introduce bias. Additionally, most patients were receiving systemic treatment at the time of imaging, complicating the interpretation of findings and making it difficult to distinguish disease-related changes from treatment effects. Finally, few studies investigated the ocular impact of specific therapies, including TTR stabilizers and gene-silencing agents.

CONCLUSIONS

While individual OCT and OCT-A parameters such as ONL thinning, CVI reduction, or SCP/DCP vessel loss are not specific to ATTR, their consistent alteration across studies highlights potential utility in a multimodal imaging approach. Combining structural and vascular markers—such as ONL thickness, pRNFL, and SFCT—may enhance diagnostic sensitivity and allow for stratification of ocular or systemic disease severity. This integrated approach could facilitate earlier detection, particularly in pre-symptomatic carriers, and support longitudinal monitoring of disease progression or treatment response. Future prospective studies should explore composite OCT/OCT-A indices

to validate their prognostic value and clinical applicability in ATTR management; however, this effort will require standardized imaging protocols, larger multicenter cohorts, and dedicated evaluations of treatment effects to ensure reliable translation into clinical practice.

ACKNOWLEDGEMENTS

The authors would like to express their sincere gratitude to Professor Demetrios G. Vavvas and Dr. Gustavo Sakuno from the Department of Ophthalmology, Massachusetts Eye and Ear, Harvard Medical School, for their valuable recommendations and expert insights, which significantly enhanced the overall quality and clarity of the manuscript.

Medical Writing/Editorial Assistance. During the preparation of this manuscript, the authors utilized ChatGPT-4.0 to enhance the readability and language. Following its use, the authors thoroughly reviewed and edited the content as necessary and accept full responsibility for the final version of the publication.

Author Contributions. Makan Ziafati and Costanza Barresi contributed to the conception and design of the study, performed literature screening and data extraction, and were involved in drafting the manuscript. Chiara Giuffrè and Maria Vittoria Cicinelli contributed to the study design, provided supervision throughout the research process, and assisted in drafting and refining the manuscript.

Funding. No funding or sponsorship was received for this study or publication of this article.

Data Availability. The data supporting the findings of this study are available from the corresponding author upon reasonable request.

Declarations

Conflict of Interest. Makan Ziafati, Costanza Barresi, Chiara Giuffrè, and Maria Vittoria Cicinelli have nothing to disclose.

Ethical Approval. This study is based on previously published literature and does not involve any new investigations involving human participants or animals; therefore, ethical approval was not required.

REFERENCES

1. Lachmann HJ, Hawkins PN. Systemic amyloidosis. Curr Opin Pharmacol. 2006;6(2):214–20.
2. Merlini G. Systemic amyloidosis: are we moving ahead. Neth J Med. 2004;62(4):104–5.
3. Violaine PB, Violaine P-B, Gérard S, Gérard S, Gérard S. Familial amyloid polyneuropathy. Lancet Neurol. 2011.
4. Wechalekar AD, Gillmore JD, Hawkins PN. Systemic amyloidosis. Lancet. 2016;387(10038):2641–54.
5. Latasiewicz M, Sala-Puigdollers A, Gonzalez-Ventosa A, Milla E, Adan Civera A. Multimodal retinal imaging of familial amyloid polyneuropathy. Ophthalmic Genet. 2019;40(5):407–20.

6. Richardson SJ. Cell and molecular biology of transthyretin and thyroid hormones. Int Rev Cytol. 2007;258:137–93.

7. Ueda M. Transthyretin: its function and amyloid formation. Neurochem Int. 2022;155:105313.

8. Frizziero L, Salvalaggio A, Cosmo E, Cipriani A, Midena E, Briani C. Ophthalmological involvement in wild-type transthyretin amyloidosis: a multimodal imaging study. J Peripher Nerv Syst. 2023;28(4):586–96.

9. Koike H, Ikeda S, Takahashi M, et al. Schwann cell and endothelial cell damage in transthyretin familial amyloid polyneuropathy. Neurology. 2016;87(21):2220–9.

10. Koike H, Misu K, Sugiura M, et al. Pathology of early- vs late-onset TTR Met30 familial amyloid polyneuropathy. Neurology. 2004;63(1):129–38.

11. David HA, David A, David HA, et al. Hereditary transthyretin amyloidosis: a model of medical progress for a fatal disease. Nat Rev Neurol. 2019;15(7):387–404.

12. Minnella AM, Rissotto R, Maceroni M, et al. Ocular involvement in hereditary transthyretin amyloidosis: a case series describing novel potential biomarkers. Genes. 2021. https://doi.org/10.3390/genes12060927.

13. Maurer MS, Bokhari S, Damy T, et al. Expert consensus recommendations for the suspicion and diagnosis of transthyretin cardiac amyloidosis. Circ Heart Fail. 2019;12(9):e006075.

14. Rinaldi M, Tranfa F, Chiosi F, et al. OCT angiography indices and the choroidal vascularity index in wild-type transthyretin (TTR) amyloidosis (ATTRwt). Front Med (Lausanne). 2023;10:1174643.

15. Vergaro G, Solal AC, Emdin M. Wild type transthyretin amyloidosis: don't miss diagnosis! Int J Cardiol. 2020;312:96–7.

16. Reynolds MM, Veverka KK, Gertz MA, et al. Ocular manifestations of familial transthyretin amyloidosis. Am J Ophthalmol. 2017;183:156–62.

17. Luigetti M, Conte A, Del Grande A, et al. TTR-related amyloid neuropathy: clinical, electrophysiological and pathological findings in 15 unrelated patients. Neurol Sci. 2013;34(7):1057–63.

18. Eiko A, Eiko A, Yukio A, et al. Ocular manifestations of familial amyloidotic polyneuropathy type I: long term follow up. British J Ophthalmol. 1997;81(4):295–8.

19. Haraoka K, Ando Y, Ando E, et al. Amyloid deposition in ocular tissues of patients with familial amyloidotic polyneuropathy (FAP). Amyloid. 2002;9(3):183–9.

20. Beirão JM, Malheiro J, Lemos C, et al. Impact of liver transplantation on the natural history of oculopathy in Portuguese patients with transthyretin (V30M) amyloidosis. Amyloid. 2015;22(1):31–5.

21. Marta A, Marques JH, Ferreira A, Coelho J, Beirão JM. Choroidal involvement in hereditary transthyretin amyloidosis patients. Retina. 2022;42(4):775–81.

22. Beirão JM, Malheiro J, Lemos C, Beirão I, Costa P, Torres P. Ophthalmological manifestations in hereditary transthyretin (ATTR V30M) carriers: a review of 513 cases. Amyloid. 2015;22(2):117–22.

23. Luigetti M, Romano A, Di Paolantonio A, Bisogni G, Sabatelli M. Diagnosis and treatment of hereditary transthyretin amyloidosis (hATTR) polyneuropathy: current perspectives on improving patient care. Ther Clin Risk Manag. 2020;16:109–23.

24. Conceição I, Damy T, Romero M, et al. Early diagnosis of ATTR amyloidosis through targeted follow-up of identified carriers of TTR gene mutations. Amyloid. 2019;26(1):3–9.

25. Page MJ, McKenzie JE, Bossuyt PM, et al. The PRISMA 2020 statement: an updated guideline for reporting systematic reviews. Br Med J. 2021;372:n71.

26. Stang A. Critical evaluation of the Newcastle-Ottawa scale for the assessment of the quality of nonrandomized studies in meta-analyses. Eur J Epidemiol. 2010;25(9):603–5.

27. NHLBI, NIH. Study quality assessment tools. Updated July 2021 [Available from: https://www.nhlbi.nih.gov/health-topics/study-quality-assessment-tools.

28. Kakihara S, Hirano T, Kitahara J, et al. Application of optical coherence tomography angiography to assess systemic severity in patients with hereditary transthyretin amyloidosis. PLoS One. 2022;17(9):e0275180.

29. Marques JH, Coelho J, Malheiro J, Pessoa B, Beirão JM. Subclinical retinal angiopathy associated with hereditary transthyretin amyloidosis—assessed with optical coherence tomography angiography. Amyloid. 2021;28(1):66–71.

30. Ruiz-Medrano J, Puertas M, Almazán-Alonso E, et al. Ophthalmologic involvement in patients

with hereditary transthyretin amyloidosis. Retina. 2023;43(1):49–56.

31. Maceroni M, Falsini B, Luigetti M, et al. Ocular morpho-functional evaluation in ATTRv pre-symptomatic carriers: a case series. Diagnostics. 2023. https://doi.org/10.3390/diagnostics13030359.

32. Marques JH, Coelho J, Malheiro J, Pessoa B, Beirão JM. Subclinical retinal angiopathy associated with hereditary transthyretin amyloidosis–assessed with optical coherence tomography angiography. Amyloid. 2021;28(1):66–71.

33. Cicinelli MV, Rabiolo A, Marchese A, et al. Choroid morphometric analysis in non-neovascular age-related macular degeneration by means of optical coherence tomography angiography. Br J Ophthalmol. 2017;101(9):1193–200.

34. Yavuzer K, Bozkurt B, Ozturk BT, Okudan S. The effect of age on subfoveal choroidal thickness in healthy subjects. East J Med. 2021;26(4):519–25.

35. Ghassemi F, Mirshahi R, Bazvand F, Fadakar K, Faghihi H, Sabour S. The quantitative measurements of foveal avascular zone using optical coherence tomography angiography in normal volunteers. J Curr Ophthalmol. 2017;29(4):293–9.

36. Shiihara H, Terasaki H, Sonoda S, et al. Objective evaluation of size and shape of superficial foveal avascular zone in normal subjects by optical coherence tomography angiography. Sci Rep. 2018;8(1):10143.

37. Falls HF, Jackson J, Carey JH, Rukavina JG, Block WD. Ocular manifestations of hereditary primary systemic amyloidosis. AMA Arch Ophthalmol. 1955;54(5):660–4.

38. Dwork AJ, Cavallaro T, Martone RL, Goodman DS, Schon EA, Herbert J. Distribution of transthyretin in the rat eye. Invest Ophthalmol Vis Sci. 1990;31(3):489–96.

39. Kawaji T, Ando Y, Nakamura M, et al. Ocular amyloid angiopathy associated with familial amyloidotic polyneuropathy caused by amyloidogenic transthyretin Y114C. Ophthalmology. 2005;112(12):2212.

40. Noble KG. Bilateral multifocal retinal arteriolar sheathing as the only ocular finding in hereditary amyloidosis. Am J Ophthalmol. 1998;125(1):111–3.

41. Rousseau A, Terrada C, Touhami S, et al. Angiographic signatures of the predominant form of familial transthyretin amyloidosis (Val30Met Mutation). Am J Ophthalmol. 2018;192:169–77.

42. Schwartz MF, Green WR, Michels RG, Kincaid MC, Fogle J. An unusual case of ocular involvement in primary systemic nonfamilial amyloidosis. Ophthalmology. 1982;89(4):394–401.

43. Yoshinaga T, Nakazato M, Ikeda S, Ohnishi A. Three siblings homozygous for the transthyretin-Met30 gene in familial amyloidotic polyneuropathy–evaluation of their clinical pictures with reference to those of other 10 cases reported. Rinsho Shinkeigaku Clin Neurol. 1994;34(2):99–105.

44. Koike H, Katsuno M. Transthyretin amyloidosis: update on the clinical spectrum, pathogenesis, and disease-modifying therapies. Neurol Ther. 2020;9(2):317–33.

45. Alber J, Arthur E, Goldfarb D, et al. The relationship between cerebral and retinal microbleeds in cerebral amyloid angiopathy (CAA): a pilot study. J Neurol Sci. 2021;423:117383.

46. Ellie E, Camou F, Vital A, et al. Recurrent subarachnoid hemorrhage associated with a new transthyretin variant (Gly53Glu). Neurology. 2001;57(1):135–7.

47. Petersen R, Goren H, Cohen M, et al. Transthyretin amyloidosis: a new mutation associated with dementia. Ann Neurol. 1997;41(3):307–13.

48. Bodez D, Guellich A, Kharoubi M, et al. Prevalence, severity, and prognostic value of sleep apnea syndromes in cardiac amyloidosis. Sleep. 2016;39(7):1333–41.

49. Dunlop AA, Graham SL. Familial amyloidotic polyneuropathy presenting with rubeotic glaucoma. Clin Experiment Ophthalmol. 2002;30(4):300–2.

50. Rapezzi C, Merlini G, Quarta CC, et al. Systemic cardiac amyloidoses: disease profiles and clinical courses of the 3 main types. Circulation. 2009;120(13):1203–12.

51. Ruberg FL, Berk JL. Transthyretin (TTR) cardiac amyloidosis. Circulation. 2012;126(10):1286–300.

52. Agrawal R, Gupta P, Tan K-A, Cheung CMG, Wong T-Y, Cheng C-Y. Choroidal vascularity index as a measure of vascular status of the choroid: measurements in healthy eyes from a population-based study. Sci Rep. 2016;6(1):21090.

53. Benson MD, Kincaid JC. The molecular biology and clinical features of amyloid neuropathy. Muscle Nerve Offic J Am Assoc Electrodiagn Med. 2007;36(4):411–23.

54. Plante-Bordeneuve V. Update in the diagnosis and management of transthyretin familial amyloid polyneuropathy. J Neurol. 2014;261(6):1227–33.

55. Kakihara S, Hirano T, Kitahara J, et al. Ocular angiographic features in Japanese patients with val30met hereditary transthyretin amyloidosis. Retina. 2022;42(1):210–5.

56. Jones L, Skara J, Cohen A, Harding J, Milunsky A, Skinner M. Familial amyloidotic polyneuropathy: a new transthyretin position 30 mutation (alanine for valine) in a family of German descent. Clin Genet. 1992;41(2):70–3.

57. Mascalchi M, Salvi F, Pirini M, et al. Transthyretin amyloidosis and superficial siderosis of the CNS. Neurology. 1999;53(7):1498.

58. Muller KR, Padbury R, Jeffrey GP, et al. Poor outcome after liver transplantation for transthyretin amyloid neuropathy in a family with an Ala36Pro transthyretin mutation: case report. Liver Transpl. 2010;16(4):470–3.

59. Zou X, Dong F, Zhang S, Tian R, Sui R. Transthyretin Ala36Pro mutation in a Chinese pedigree of familial transthyretin amyloidosis with elevated vitreous and serum vascular endothelial growth factor. Exp Eye Res. 2013;110:44–9.

60. Waddington-Cruz M, Schmidt H, Botteman MF, et al. Epidemiological and clinical characteristics of symptomatic hereditary transthyretin amyloid polyneuropathy: a global case series. Orphanet J Rare Dis. 2019;14:1–7.

61. Patel K, Hawkins P. Cardiac amyloidosis: where are we today? J Intern Med. 2015;278(2):126–44.

62. aus dem Siepen F, Hein S, Prestel S, et al. Carpal tunnel syndrome and spinal canal stenosis: harbingers of transthyretin amyloid cardiomyopathy? Clin Res Cardiol 2019;108:1324–30.

63. Wajnsztajn Yungher F, Kim A, Boehme A, et al. Peripheral neuropathy symptoms in wild type transthyretin amyloidosis. J Peripher Nerv Syst. 2020;25(3):265–72.

64. Campagnolo M, Cacciavillani M, Cipriani A, et al. Peripheral nerve involvement in wild-type transthyretin amyloidosis. Neurol Sci. 2023;44(1):351–4.

65. Rousseau A, Cauquil C, Dupas B, et al. Potential role of in vivo confocal microscopy for imaging corneal nerves in transthyretin familial amyloid polyneuropathy. JAMA Ophthalmol. 2016;134(9):983–9.

66. Fritz CD, Blaney E. Evaluation and management strategies for GI involvement with amyloidosis. Am J Med. 2022;135:S20–3.

67. Obici L, Suhr OB. Diagnosis and treatment of gastrointestinal dysfunction in hereditary TTR amyloidosis. Clin Auton Res. 2019;29(Suppl 1):55–63.

68. Wixner J, Mundayat R, Karayal ON, Anan I, Karling P, Suhr OB. Thaos: gastrointestinal manifestations of transthyretin amyloidosis-common complications of a rare disease. Orphanet J Rare Dis. 2014;9:1–9.

69. Bulawa CE, Connelly S, Devit M, et al. Tafamidis, a potent and selective transthyretin kinetic stabilizer that inhibits the amyloid cascade. Proc Natl Acad Sci U S A. 2012;109(24):9629–34.

70. Colon W, Kelly JW. Partial denaturation of transthyretin is sufficient for amyloid fibril formation in vitro. Biochemistry. 1992;31(36):8654–60.

71. Mathew SM, Mathew SM, Jeffrey HS, et al. Tafamidis Treatment for patients with transthyretin amyloid cardiomyopathy. N Engl J Med 2018.

72. Russo M, Gentile L, Toscano A, Aguennouz M, Vita G, Mazzeo A. Advances in treatment of ATTRv amyloidosis: state of the art and future prospects. Brain Sci. 2020. https://doi.org/10.3390/brainsci10120952.

73. Coelho T, Maia LF, da Silva AM, et al. Long-term effects of tafamidis for the treatment of transthyretin familial amyloid polyneuropathy. J Neurol. 2013;260(11):2802–14.

74. Coelho T, Maia LF, Martins da Silva A, et al. Tafamidis for transthyretin familial amyloid polyneuropathy: a randomized, controlled trial. Neurology. 2012;79(8):785–92.

75. Coelho T, Merlini G, Bulawa CE, et al. Mechanism of action and clinical application of tafamidis in hereditary transthyretin amyloidosis. Neurol Ther. 2016;5:1–25.

76. Buxbaum JN, Brannagan T III, Buades-Reinés J, et al. Transthyretin deposition in the eye in the era of effective therapy for hereditary ATTRV30M amyloidosis. Amyloid. 2019;26(1):10–4.

77. Monteiro C, Martins da Silva A, Ferreira N, et al. Cerebrospinal fluid and vitreous body exposure to orally administered tafamidis in hereditary ATTRV30M (p. TTRV50M) amyloidosis patients. Amyloid. 2018;25(2):120–8.

78. Adams D, Gonzalez-Duarte A, O'Riordan WD, et al. Patisiran, an RNAi therapeutic, for hereditary transthyretin amyloidosis. N Engl J Med. 2018;379(1):11–21.

79. Coelho T, Adams D, Silva A, et al. Safety and efficacy of RNAi therapy for transthyretin amyloidosis. N Engl J Med. 2013;369(9):819–29.

80. Ioannou A, Fontana M, Gillmore JD. RNA targeting and gene editing strategies for transthyretin amyloidosis. BioDrugs. 2023;37(2):127–42.

81. Ticau S, Aldinc E, Polydefkis M, et al. Treatment response and neurofilament light chain levels with long-term patisiran in hereditary transthyretin-mediated amyloidosis with polyneuropathy: 24-month results of an open-label extension study. Amyloid. 2024;31(1):1–11.

82. Adams D, Polydefkis M, González-Duarte A, et al. Long-term safety and efficacy of patisiran for hereditary transthyretin-mediated amyloidosis with polyneuropathy: 12-month results of an open-label extension study. Lancet Neurol. 2021;20(1):49–59.

83. David HA, David A, David A, et al. Patisiran, an RNAi therapeutic, for hereditary transthyretin amyloidosis. N Engl J Med 2018.

84. Solomon SD, Adams D, Kristen A, et al. Effects of patisiran, an RNA interference therapeutic, on cardiac parameters in patients with hereditary transthyretin-mediated amyloidosis: analysis of the APOLLO study. Circulation. 2019;139(4):431–43.

85. Benson MD. Liver transplantation and transthyretin amyloidosis. Muscle Nerve. 2013;47(2):157–62.

86. Suhr OB, Herlenius G, Friman S, Ericzon BG. Liver transplantation for hereditary transthyretin amyloidosis. Liver Transpl. 2000;6(3):263–76.

87. Carvalho A, Rocha A, Lobato L. Liver transplantation in transthyretin amyloidosis: issues and challenges. Liver Transpl. 2015;21(3):282–92.

88. Ando Y, Terazaki H, Nakamura M, et al. A different amyloid formation mechanism: de novo oculoleptomeningeal amyloid deposits after liver transplantation. Transplantation. 2004;77(3):345–9.

89. João Melo B, João Melo B, Jorge M, et al. Impact of liver transplantation on the natural history of oculopathy in Portuguese patients with transthyretin (V30M) amyloidosis. Amyloid. 2015.

90. Kawaji T, Ando Y, Nakamura M, et al. Transthyretin synthesis in rabbit ciliary pigment epithelium. Exp Eye Res. 2005;81(3):306–12.

91. Ryuhei H, Ryuhei H, Takahiro K, et al. Impact of liver transplantation on transthyretin-related ocular amyloidosis in Japanese patients. Arch Ophthalmol 2010.

92. Sandgren O, Kjellgren D, Suhr OB. Ocular manifestations in liver transplant recipients with familial amyloid polyneuropathy. Acta Ophthalmol. 2008;86(5):520–4.

93. Schmidt HH, Wixner J, Planté-Bordeneuve V, et al. Patisiran treatment in patients with hereditary transthyretin-mediated amyloidosis with polyneuropathy after liver transplantation. Am J Transplant. 2022;22(6):1646–57.